

## $\kappa$ -Opioid Receptor Model in a Phospholipid Bilayer: Molecular Dynamics Simulation

Manuela Iadanza,<sup>†</sup> Monika Höltje,<sup>‡</sup> Giuseppe Ronsisvalle,<sup>†</sup> and Hans-Dieter Höltje\*<sup>§</sup>

Department of Pharmaceutical Sciences, University of Catania, Viale Andrea Doria, 6, 95125 Catania, Italy, Research Centre Jülich IBI-2, D-52425 Jülich, Germany, and Institute of Pharmaceutical Chemistry, Heinrich-Heine-Universität, Universitätsstrasse 1, D-40225 Düsseldorf, Germany

Received April 18, 2002

A three-dimensional molecular model of the transmembrane domain of the  $\kappa$ -opioid receptor in a phospholipid bilayer is presented. The endogenous ligand, dynorphin A (**1**), and synthetic ligands, benzomorphan-based compounds (**2a**, **2b**) (Figure 1), are docked into the model. We report the results of a 500 ps molecular dynamics simulation of these protein–ligand complexes in a simplified bilayer of 97 molecules of the lipid dipalmitoylphosphatidylcholine and 26 water molecules per lipid. The simulations explore the stability and conformational dynamics of the model in a phospholipid bilayer; we also investigate the interactions of the protein with its ligands. Molecular simulation of the receptor–ligand complexes, endogenous and synthetic, has confirmed the existence of different binding domains for peptide and non-peptide ligands. Similarities are found in the dynamics and binding mode of all conformations of the synthetic ligands studied. The protonated hydrogen of the benzomorphan is always involved in an H-bond with Asp138, and other potentially stabilizing receptor–ligand interactions found involve the hydroxyl substituent on the benzomorphan, which may form an H-bond with Tyr139 or Gly190 according to the different molecules. The ester group of **2a** may therefore form an H-bond with Ile316, while the carbonyl group of **2b** forms an H-bond with Gln115 and Tyr312. The remaining part of the ligand is located in the extracellular portion of the pocket. It is surrounded by hydrophobic residues in the transmembrane region (TM), and it interacts with different sets of residues. The results obtained are in general agreement with site-directed mutagenesis data that have highlighted the importance of all TM regions for synthetic-ligand affinity with the  $\kappa$ -opioid receptor.

### Introduction

Three types of opioid receptor, known as  $\mu$ ,  $\delta$ , and  $\kappa$ , recently identified and cloned<sup>1</sup> have attracted a considerable attention to the chemistry of opioid proteins. The physiological effects associated with opiate use are widely varied and include analgesia, euphoria, sedation, respiratory depression, changes in thermoregulation, inhibition of gastrointestinal motility, muscle rigidity, and the potential for physical dependence and abuse. These physiological effects are controlled by the activity of specific G-protein-coupled receptors (GPCRs) that bind opioids. Therefore, these receptors have been classified as members of the superfamily of G-protein-coupled receptors.

The GPCRs consist of integral membrane proteins. The function of such proteins is to transduce a chemical signal across a cell membrane, allowing communication between the exterior and the interior of the cell.<sup>2</sup> Actually GPCRs bind to cytoplasmic, trimeric proteins called G-proteins, consisting of  $\alpha$ ,  $\beta$ , and  $\gamma$  subunits, to mediate signaling pathways inside the cell. When the appropriate ligand is bound by a GPCR at the extracellular face of the membrane, a biochemical event

occurs inside the cell. Although the receptors of this type share a common 3D structure, they have a different sequence of amino acids responsible for protein activation by specific signals. They consist of a single polypeptide chain containing seven helical transmembrane domains (TM I–VII) arranged in a fairly close-packed bundle connected by three extracellular and three intracellular loops outside the lipid membrane.

Intensive studies of the site-directed mutagenesis of the GPCR family, the application of alignment techniques, and homology modeling approaches have made it possible to build different GPCR molecular models.<sup>3,4</sup> It can help to predict the role of different residues on binding and the importance of some residues for receptor functionality, as well as to understand different ligand binding modes and selectivity, providing insights into the design of new synthetic compounds with various degrees of receptor selectivity.

Naturally, different levels of approximation are necessary in the simulations to build a receptor model. Thus, to reduce the inherent conformational flexibility in peptides, it may be sufficient to run simulations in which the proteins are gently restrained, but in this way, the bilayer environment of the protein is fully omitted. Therefore, understanding the restriction imposed by the lipid bilayer environment on membrane protein structure and dynamics is needed for the successful prediction of membrane protein tertiary struc-

\* To whom correspondence should be addressed. Phone: +49 211 81 13661. Fax: +49 211 81 13847. E-mail: hoeltje@pharm.uni-duesseldorf.de.

<sup>†</sup> University of Catania.

<sup>‡</sup> Research Centre Jülich.

<sup>§</sup> Heinrich-Heine University.

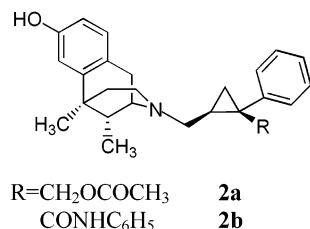


**Figure 1.** Endogenous ligand dynorphin A and synthetic ligands, benzomorphan-based compounds, used in the study.

ture. Certainly this coupling between environment and protein gives a more dynamic aspect of the system.

At present, a detailed consideration of simplified model systems can give molecular insight into motions and interactions that will be present in larger, more complex systems as well as provide details important for a discussion of protein folding. Consequently we decided to examine the conformations of the  $\kappa$ -opioid receptor with its ligands that are stabilized in the context of a model membrane that closely resembles the chemical environment that a peptide may encounter *in vivo*.

We used an available model of  $\kappa$ -opioid receptor recently reported by Metzger and co-workers consisting of TM (I–VII) and the second extracellular loop (EL2).<sup>5</sup> This model is unique in that the secondary structures are taken from nonsequential alignments to the helical domains of bacteriorhodopsin,<sup>6</sup> thus allowing the conformational effects of the conserved prolines to be retained, while the helix packing orientations and the lengths were modified using the sequence analysis of the projection structure of rhodopsin.<sup>7,8</sup>

A comparison of this model with another model based on the rhodopsin template introduced by Baldwin some time ago<sup>9</sup> shows little difference in the orientation of the helices in the transmembrane domains; however, the superimposition of the residues of the hypothetical binding pocket is well-conserved.

The crystal coordinates of bovine rhodopsin were not available at this time.<sup>10</sup> Whether the use of these coordinates would improve the current receptor model structure remains to be clarified.

The aim of our study is to extend this model by molecular dynamics simulations of the  $\kappa$ -opioid receptor in a simplified bilayer environment. In other words, the protein has to be introduced into a more natural environment, avoiding use of any artificial restraints. The endogenous ligand dynorphin A (dynA), consisting of amino acids 1–10, and the benzomorphan-based synthetic ligands, synthesized by Ronsisvalle and co-workers<sup>11</sup> (Figure 1), were docked into the model of  $\kappa$ -opioid receptor to investigate the behavior of the protein–ligand system inside a bilayer.

Affinity data of the ligands and references are given in Table 1.

## Experimental Section

**Methods.** The computations were performed on a SGI Indigo2 or a SGI Origin 2000 workstation (Silicon Graphics, Inc., Mountain View, CA)

**Protein.** The protein coordinates of  $\kappa$ -opioid receptor from Metzger's model were tested with the PROCHECK computer program.<sup>12</sup> It was slightly modified during a minimization procedure and subsequently used as the starting structure for ligand docking studies.

**Table 1.** Binding Affinity Data of Compounds **2a**, **2b**, and MPCB

compound	$K_i$ (nM)	ref
<b>2a</b>	228 <sup>a</sup>	10
<b>2b</b>	2355 <sup>a</sup>	10
MPCB	240 <sup>b</sup>	12

<sup>a</sup> Inhibition of [<sup>3</sup>H]U69593 binding in guinea pig brain homogenates. <sup>b</sup> Inhibition of [<sup>3</sup>H]diprenorphine binding in guinea pig cerebella fraction.

**Ligands.** The ligands used in this study were the endogenous dynA and the two synthetic compounds, benzomorphan derivatives, prepared by Ronsisvalle's group<sup>11</sup> (Figure 1). These synthetic ligands were taken from the series of compounds synthesized to perform structure–activity relationship (SAR) studies on MPCB, [(–)-*R,S*-6,11-dimethyl-1,2,3,4,5,6-hexahydro-3-[(2'-methoxycarbonyl-2'-phenylcyclopropyl)methyl]-2,6-methano-3-benzazocin-8-ol], found to be a specific  $\kappa$ -opioid agonist.<sup>13</sup>

The coordinates of dynA were taken from the two-dimensional NMR study reported by Tessmer and Kallick.<sup>14</sup> The computer models of the two benzomorphan derivatives were built using the fragment libraries available in the molecular modeling software package SYBYL.<sup>15</sup> Ligands were modeled in their nitrogen-protonated form. The initial structures, thus obtained, were subsequently used for geometry optimization and energy minimization employing a conjugate gradient method<sup>16</sup> and the semiempirical AM1 algorithm.<sup>17</sup> A systematic conformational search for low-energy conformations was performed by applying the SEARCH option within the SYBYL program. The TRIPOS force field was used.<sup>18</sup> Calculations were carried out under vacuum conditions, neglecting electrostatic interactions. Flexible bonds were fully rotated with rotational increments of 10°. Conformations with an energy higher than 10 kcal/mol above the absolute energy minimum were discarded. The remaining conformers were grouped into common families belonging to identical local minima, using IXGROS computer program.<sup>19</sup> Among the resulting conformations, only those associated with more energetically favorable values (three for **2a** and three for **2b**) were further evaluated for their ability to fit the  $\kappa$ -opioid receptor model by docking studies.

**Ligand Docking.** All three conformers of both compounds were superimposed on dynA (Figure 2). These conformers mimic the first amino acids of the endogenous ligand; therefore, we docked them to the receptor model, keeping the specific interactions between the amino acids of the receptor and the corresponding functional groups of dynA (analogous with our ligands) as proposed by Paterlini et al.<sup>20</sup> The specific interactions include H-bonds and  $\pi$ – $\pi$  interactions through the first amino acid of dynA, Tyr1. It was found that the carboxyl group of the Asp138 (TM III) is responsible for the most important H-bond ligand–receptor interaction. The importance of this binding has been demonstrated by mutagenesis studies.<sup>21,22</sup>

Consequently in every docking model the protonated nitrogen of Tyr1 of dynA or the protonated nitrogen of the benzomorphan part of the ligands was positioned in such a way that it can interact with the carboxyl group of Asp138.

The docking of our compounds was performed in two steps. First, the phenol ring and the protonated nitrogen of the benzomorphan part were placed in the binding pocket to provide the most effective  $\pi$ – $\pi$  interactions with appropriate aromatic amino acids and H-bonding interactions with Asp138, while the rest of the molecule was oriented toward the extracellular surface. Second, the spatial positions of the different ligand conformations were adjusted to exclude all hindrances with the receptor atoms and to form additional H-bonds and hydrophobic interactions in the binding pocket. Finally, the ligand and the interacting part of the receptor were optimized with the Powell conjugate gradient method with neglect of electrostatics to remove sterically unfavorable interactions from docking.

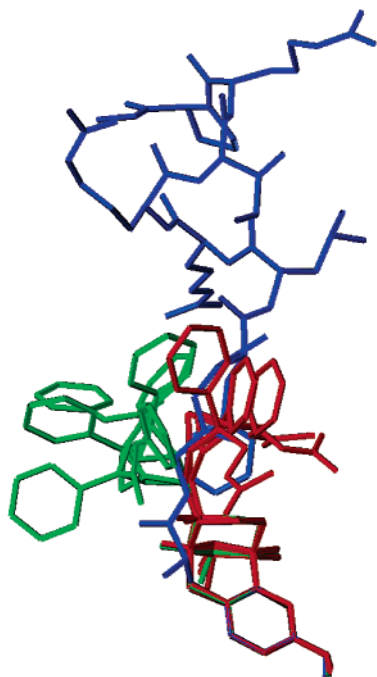


**Figure 2.** Superimposition of all the conformations of the synthetic ligand on dynorphin A (1–10): (red) **2a**; (green) **2b**.

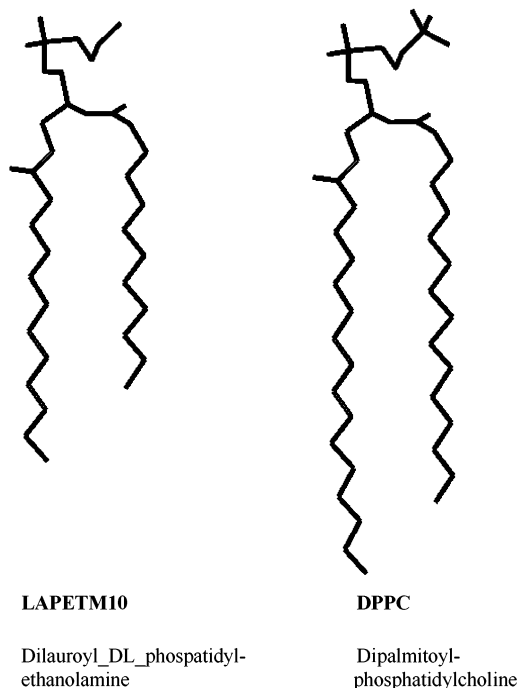


**Figure 3.** Crystal structure of dilauroyl-DL-phosphatidylethanolamine (LAPETM10) and modeling structure of dipalmitoylphosphatidylcholine (DPPC).

**Bilayer.** The bilayer system was built from the crystal structure of 1,2-dilauroyl-DL-phosphatidylethanolamine (acetic acid solvate)<sup>23</sup> taken from Cambridge Structural Database (CSD) (refcode lapetm10).<sup>24</sup> We modified the length of the chains and the headgroup of this molecule to result in the dipalmitoylphosphatidylcholine (DPPC) molecule (Figure 3). The CRYGIN option of the SYBYL program was used to obtain the required extension of the bilayer suitable for protein accommodation. The bilayer system was relaxed by energy minimization with steepest descent algorithm. However, available crystal structures of phospholipid molecules do not provide convenient configurations that can be used as building blocks to assemble the protein membrane system.<sup>25</sup> At physiological

temperature, hydrated phospholipid bilayers are in a partly ordered, partly disordered dynamic liquid-crystalline state. This means that the bilayer adopts the liquid-crystalline phase ( $L_{\alpha}$  state) associated with disorder and a mixture of trans, gauche, and kinked alkyl chains. Because the alkyl chains of the DPPC crystal at low temperature are in an all-trans conformation, similar to that of the gel state,<sup>26</sup> the state of the starting system, constructed from the X-ray structure of phospholipid, differs markedly from that of an equilibrated liquid-crystalline bilayer; thus, a significant amount of computer time will be required to melt the all-trans alkyl chains. Therefore, it is desirable to start the simulation of the protein-membrane system from a configuration that corresponds as closely as possible to the liquid-crystalline state of the bilayer to reduce the computer time needed for equilibration.<sup>27</sup> This allows a much more rapid approach to a realistic starting point than is possible with gel state starting conditions.

Consequently, to avoid these difficulties, because of the handmade nature of our initial structure, the bilayer system was preequilibrated by a short molecular dynamics (MD) run (99 ps), obtaining in this way a lipid arrangement representative of the liquid-crystalline state. This supports a more rapid relaxation than would a start from an all-trans conformation as suggested by Heller et al.<sup>28</sup> The  $\kappa$ -receptor model with the different ligands was placed into the bilayer structure in such a way that the ends of the helices were approximately coincident with the bilayer-water interfaces and that the long axes of the helices were perpendicular to the bilayer; the positions of the helix axes and their orientations with respect to the membrane plane were then adjusted as proposed by Baldwin.<sup>9</sup> DPPC molecules overlapping with the peptide were removed. The side chains of the protein of the resulting system were energy-minimized with the Powell conjugate gradient method to remove all the bad contacts with the preequilibrated DPPC lipids and to increase the number of H-bonding interactions between the different side chains of amino acids and the appropriate portion of phospholipids. The system was then solvated with SPC water models, as recommended by Tieleman and Berendsen in interface membrane studies,<sup>29,30</sup> and energy-minimized.

The whole system consists of 97 DPPC molecules. The bilayer with the receptor was covered by 2573 water molecules, leading to a water slab of about 10 Å thickness from each side of the bilayer. This thickness corresponds to more than 26 water molecules per phospholipid unit, which is within the range found experimentally for the number of water molecules at saturation; NMR studies show the presence of about 20 water molecules per phospholipid molecule in the membrane.<sup>31,32</sup> The total number of atoms in the system under study, including DPPC, water, and protein, was 14 627.

**Dynamics Simulations.** Molecular dynamics simulations were performed using the GROMACS package.<sup>33,34</sup>

For all atoms, the standard parameters of the GROMACS force field were used. For the hydrocarbon chains of phospholipids, the Ryckaert-Bellemans potential was applied.<sup>35,36</sup> The Ryckaert-Bellemans potential has been proved to be more realistic for liquid alkanes because it permits an easier angle transformation from trans to gauche than using the GROMACS dihedral potential. In this way the headgroup-headgroup attractions as well as the tail-tail interactions will be lower, allowing a lateral expansion and therefore destabilization of the gel phase.

Periodic boundary conditions were applied in all three dimensions.

A twin-range cutoff of 1.0 nm was used for the Lennard-Jones and short-range Coulomb interactions and a cutoff of 1.8 nm was used for the long-range Coulomb interactions with updates every 10 steps. The time step for integration of the equations of motion was 1 fs. *NPT* conditions (constant number of particles, pressure, and temperature) were used in all our simulations. Water, lipids, protein, and ligand were coupled separately to a temperature bath at 300 K, with a coupling constant  $\tau_T = 0.1$  ps. The system was simulated at constant pressure, 1 bar in all dimensions, with a coupling constant  $\tau_P$

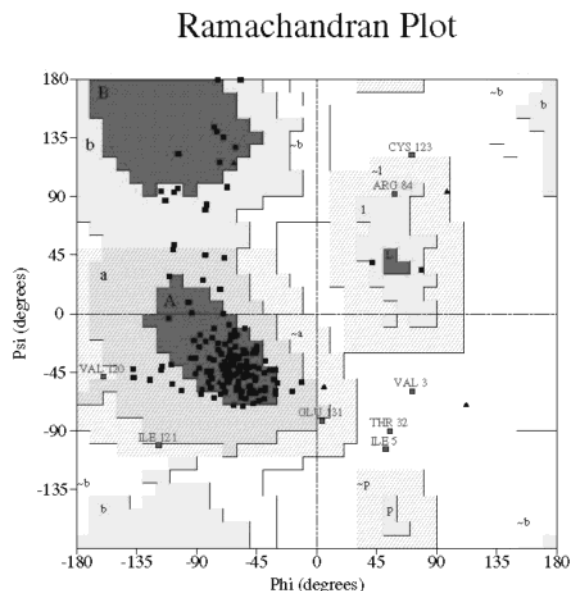


**Figure 4.** Ramachandran plot for one of the final structures produced using the program PROCHECK.

= 1.0 ps.<sup>37</sup> This allows the bilayer–peptide area to adjust to its optimum, depending of the force field employed. In practice, the fluctuations in the area during the production run were only ~1%.

The time of each computer run was 500 ps. The average structures were calculated for all the conformations from the last part of the MD simulations and were energy-minimized using the steepest descent methods available within the SYBYL program. Therefore, the final structures were analyzed using the program PROCHECK. Nearly all residues were found in the allowed regions of the Ramachandran plot with side chain dihedrals in ideal regions (Figure 4). In particular, 95% of the residues were found in the most favored region and in the additional allowed region. Only four amino acids (Val3, Ile5, Thr32, Cys123; see Ramachandran plot) are found in the disallowed regions. These amino acids are located in the solvent-exposed parts of the protein that do not have a definite secondary structure.

## Results

**Structure and Stability.** To examine the variations in the intramolecular conformations of the protein and the lipids within the complex bilayer environment, the root-mean-squared deviation (rmsd) with respect to the starting structure was calculated. Simulation time versus rmsd of the backbone of the protein during the full simulation (500 ps of molecular dynamics) with dyn A and with one conformation of **2a** is presented in Figure 5. The rmsd difference of the  $\kappa$ -opioid model with dynA as ligand was about 0.2 nm. A higher value of 0.3 nm was found for the considered conformation of **2a** as ligand. The relative magnitudes of the fluctuations were also conserved with the other systems, where the rms deviations were approximately 0.29 and 0.26 nm for the other two conformations of **2a** and 0.28, 0.26, and 0.27 for the three conformations of **2b** (data not shown for the sake of clarity). The backbone of the protein thus demonstrated a relatively small variation throughout all six systems with synthetic ligands, while the rmsd value, 0.2 nm, of the system  $\kappa$ -receptor–dynA, as we expected, is lower considering the whole analogy with the starting structure of our simulations.

In contrast, the rms differences between the lipids and their initial starting structure were larger and reached

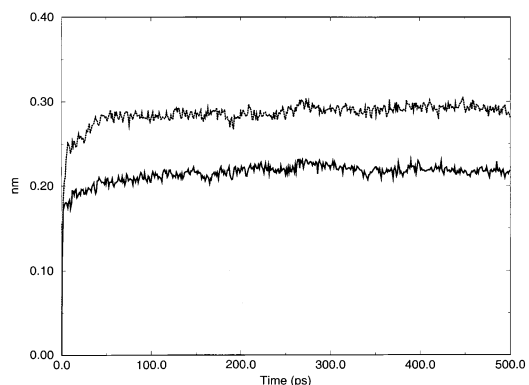


**Figure 5.** Simulation time vs rmsd of the backbones of the system with dyn A (solid line, bottom) and of the system with synthetic ligand **2a** (dotted line, top).

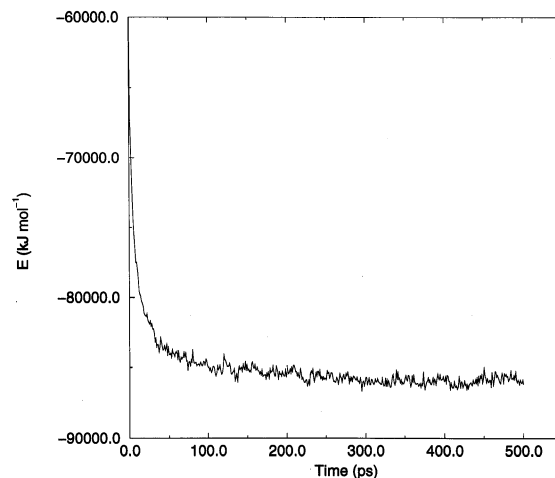


**Figure 6.** Energy variation for the systems during the simulation.

a plateau at about 2 nm. The changes in the lipid conformation will be discussed in the bilayer section.

The stability of the molecular assembly during the course of the 500 ps molecular dynamics simulations was monitored by using the same values of rms deviations. For all the systems under study, after an immediate increase of the rms deviation the characteristic steady state of protein dynamics was reached. This means that the systems were already well equilibrated after the first steps of molecular dynamics simulations.

The stability of the models obtained was evaluated with calculation of the total energy of the system as well (Figure 6). The results showed that all the models became stable after 200 ps of simulation time.

The variations along the polypeptide chain of the positional rms fluctuations of the C $\alpha$  atoms were estimated. In Figure 7 the C $\alpha$  rms fluctuations are plotted as a function of the residue number for the systems dynA–receptor (A) and BML CNF1–receptor (B). It was possible to distinguish between the different helical regions and the loop region to identify the part of the protein that was changed to the greater extent. For the dynA–receptor model, no significant variations were found; the rms value was about 0.2 nm for each part (7-TM, EL2) of the protein. For the synthetic ligands–receptor models, the rms fluctuation (about 0.2 nm) measured for the helix of each protein conformation demonstrated quite similar helices behavior, indicating

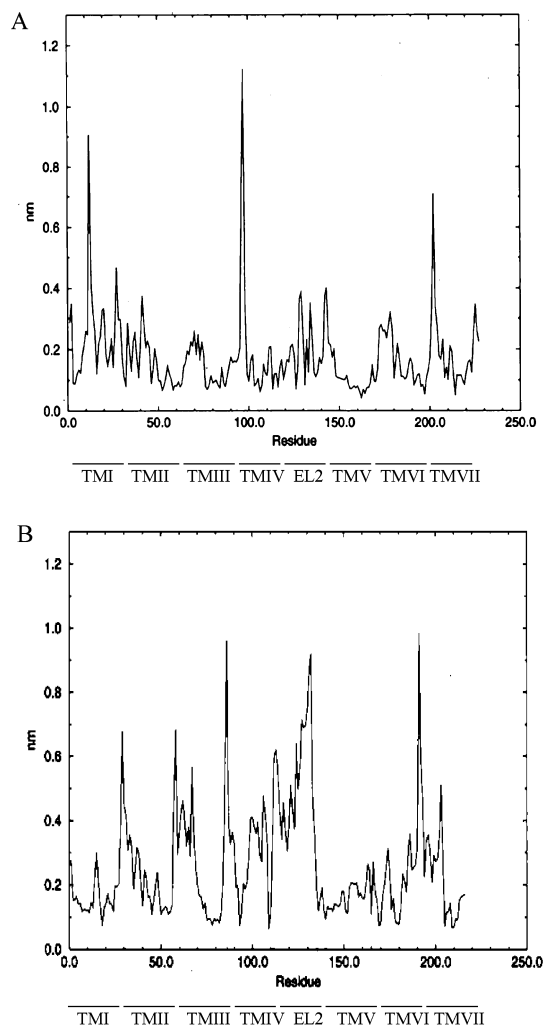


**Figure 7.** Residue-by-residue  $C\alpha$  rms fluctuations about their average coordinates for the system dynA–receptor (A) and for the system synthetic ligand–receptor (B).

the stability of 7-TM in the bilayer environment. However, the values of rms fluctuation of the EL2 region were considerably different (0.55–0.60 nm for all the conformations) from those belonging to the starting model. The main reason for this difference is that the size and the binding site of the endogenous ligand are quite unlike the synthetic one. The C-terminal part of dynA interacts with EL2 (helix–helix interaction), causing a specific conformation of the loop. Because of the lack of the interaction of the benzomorphan derivatives with the loop, EL2 undergoes different conformations changes.

The rms confirms the stability of the helices in a bilayer environment.

The possible H-bond interactions in our models between the protein and its environment, lipid and water, were evaluated. The analysis of the peptide showed that lysine side chains take extended conformation in order to maximize their contact with water and the phosphate part of the lipids. In particular, Lys60 (TM III), Lys113 (EL2), and Lys89 (TM IV) seemed to be involved in H-bonds with both lipids and water. This is in a good agreement with a simplified model of a TM helix, which shows that lysine residues at either ends of the helix interact strongly with water in the interfacial region.<sup>38</sup> Arg115 (EL2), Phe127 (EL2), Ala88 (TM IV), and Tyr9

(TM I) represent the other amino acids that interact with the lipids through H-bonds during almost the entire simulation. The protein–water H-bond interaction was the subject of a similar analysis. It was found that besides lysine residues, Val56 (TM I), Asn33 (TM II), Gly110 (TM IV), Ile183 (TM VI), Tyr195 (TM VI), and most of the amino acids of the EL2 are able to form H-bonds with water during the entire simulation. All the amino acids involved in this type of H-bond are located at both the ends of the helices or at EL2 and are therefore favorably close to the water–lipid interfaces. This is expected to contribute to the stability of the helix bundle by helping to anchor it to the lipid bilayer.

**Bilayer.** According to the literature, we used as a starting system a preequilibrated phospholipid bilayer in which we merged the protein. At the end of simulations a quite stable liquid-crystalline bilayer phase was obtained, as deduced from the calculated lipids parameters that were in agreement with previous molecular dynamics studies of lipid bilayers.<sup>39</sup> These values give a good reproduction of the experimental properties of a DPPC bilayer.<sup>40,41</sup>

A typical snapshot of the bilayer–water system along the MD trajectory is given in Figure 8. The changes in the lipid conformation are more pronounced along the alkyl chains and more modest in the polar head. From the analysis of the dynamics trajectories, it can be seen that the major axis of the lipid headgroups remains nearly parallel to the bilayer surface during the simulations. Figure 8 shows the presence of a significant amount of disorder in the fatty chain region, which is characteristic of the liquid-crystalline phase. In fact, the analysis of the rms fluctuation between the lipids and their initial starting structure (Figure 9) shows, according to above, the variation along the lipid backbone of the atoms during molecular dynamics. The high rms values, on the order of 2.0 nm for all the seven systems, confirm the changes to the liquid-crystalline state.

To quantify the dynamics of the alkyl chains of the lipids, the deuterium order parameter,  $S_{CD}$ , has been calculated.<sup>28,42</sup> This value gives a measure of the hydrocarbon chain behavior. It is possible to obtain an order parameter for every carbon position in the chains and therefore to observe the ordering behavior along the chain. Experimentally,  $S_{CD}$  is calculated from the quadrupolar splittings measured by <sup>2</sup>H NMR on phospholipids. In molecular dynamics simulation, this parameter is obtained as

$$S_{CD} = \frac{3}{2} \cos^2 \Theta - \frac{1}{2}$$

where  $\Theta$  represents the angle between the CD bond vector and the bilayer normal.

The variation of the calculated order parameter of the phospholipids in one simulation as a function of the carbon position in the two chains is shown in Figure 10. The results of the simulations differ only slightly from the others, but all show the typical variation of the curve, with a plateau over the central region of the chains extending approximately over the first 10 carbons and a decrease toward the chain end where there is the larger fraction of gauche angles. The order

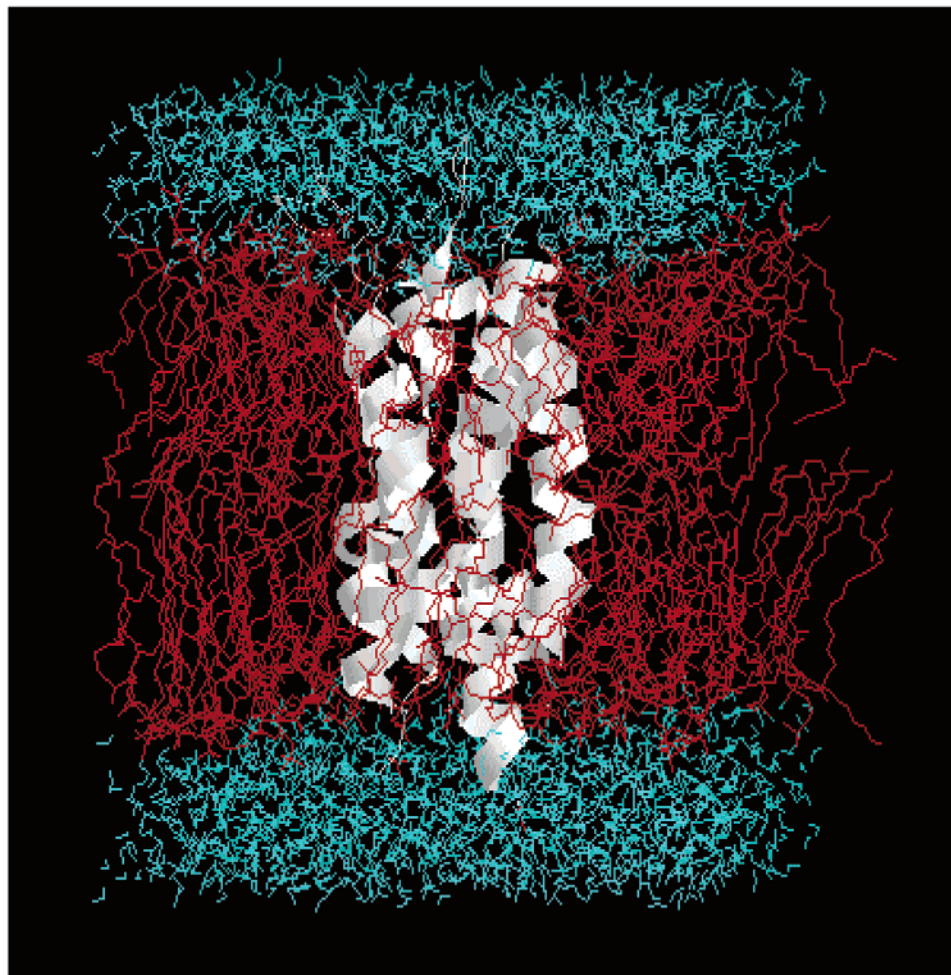


**Figure 8.** Molecular graphics view of the simulation system for the  $\kappa$ -receptor model (white) inserted in a DPPC bilayer (red) with water (cyan) on either side, after 500 ps of dynamics run. The helices of the protein are shown in ribbon format.

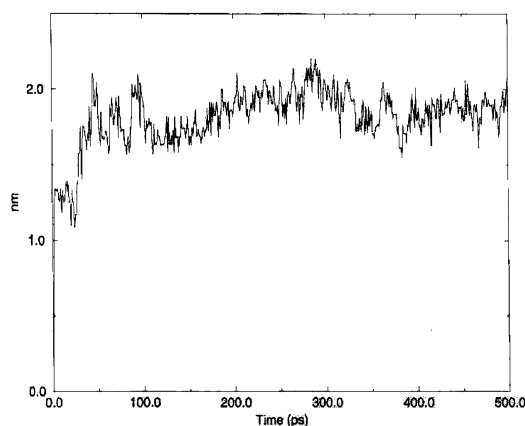


**Figure 9.** Simulation time vs rmsd of the lipids.

parameter profile for DPPC from  $^2\text{H}$  NMR measurements is reported for comparison in Figure 9.<sup>43</sup> The results of our simulations are in good agreement with the experimental values.

Our simulations were performed at 300 K, which is slightly lower than physiological temperature. Therefore, to check possible differences in the phospholipid behavior, one of the simulations was repeated at 315 K. No significant variations were found between the values of the order parameter calculated at this temperature and those at 300 K.

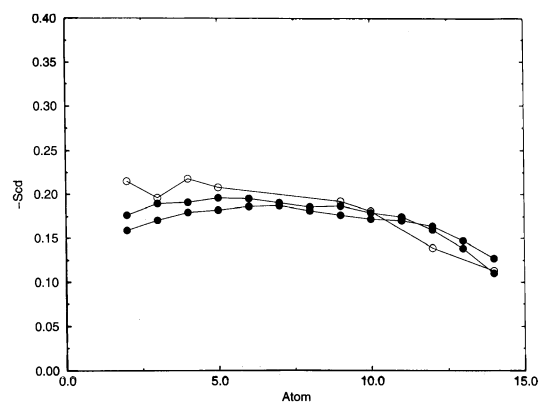


**Figure 10.** Order parameters  $-S_{\text{CD}}$  as a function of carbon atom number in the DPPC tails in the  $L_{\beta}$  phase. For comparison, the experimental values (O) are included.

**Average Structure.** A good overlap was obtained between the average structure of the  $\kappa$ -receptor model with dynA and the structure we used in our study. The turn-helix motif supposed for the N-terminal part of EL2 of the protein and the helical portion of dynA<sup>20</sup> remained unchanged throughout the simulation. Therefore, the helix-helix interactions between hydrophobic residues of EL2 (Val201, Val205, Val207, Ile208) and the hydrophobic helical components of dynA (Phe4, Leu5, Ile8), responsible for the binding, were kept. The charged amino terminus of Tyr1 forms an ion pair with

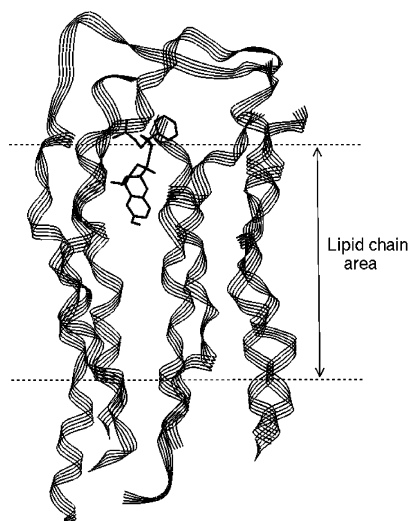


**Figure 11.** Ribbon representation of the protein together with the ligand. The TM area is marked so that it is possible to observe the relative position of the ligand.

Asp138, and its phenolic ring is also directed toward a region rich in aromatic residues such as Phe231 and Phe235 (TMV). Therefore, according to the literature, the first four amino acids of dynA were bound within the aromatic pocket in the transmembrane domain while the helical portion contacted residues in EL2 and in the extracellular end of transmembrane helices VI and VII.

An analysis of the molecular dynamics simulations of the receptor with the benzomorphan derivatives revealed similarities in the dynamics and binding modes of all the conformations of the synthetic ligands studied.

Even if the superimposition of all the average structures of all the conformations showed that they assume a different spatial disposition in the binding pocket, the part of the benzomorphan derivatives important for the binding and the corresponding residues of the protein are able to adapt to each other in such a way to permit the same interactions. In Figure 11 is shown a ribbon-representation of the protein together with the ligand; the TM area is marked, and it is possible to perceive the relative position of the ligand. The main interaction found was the H-bond between the protonated nitrogen of benzomorphan derivatives and the Asp138 (TM III) carboxylate group (Figure 12). This interaction, characteristic for all opioid ligands, is a key anchoring point for the agonist  $\kappa$ -receptor association. This correlates with mutagenesis data, which have displayed a deleterious effect of the substitution of Asp138 (TM III) on receptor activation and on the binding of agonists such as U50,488 and U69,593 (selective  $\kappa$ -agonist of the arylacetamide class).<sup>21</sup> Other potentially stabilizing receptor–ligand interactions found in this study involved the hydroxyl substituent on the benzomorphan, which may form an H-bond with Tyr139 (TM III) in the case of **2a** ligand (Figure 12) and with Gly190 (TM IV) for **2b**. The ester group of **2a** may therefore form an H-bond with Ile316 (TM VII), while the carbonyl group of **2b** forms an H-bond with Gln115 (TM II) and Tyr312 (TM VII).

Apart from these specific point interactions, the ligands are surrounded by hydrophobic residues in the TM region. In particular, the phenol ring of benzomor-

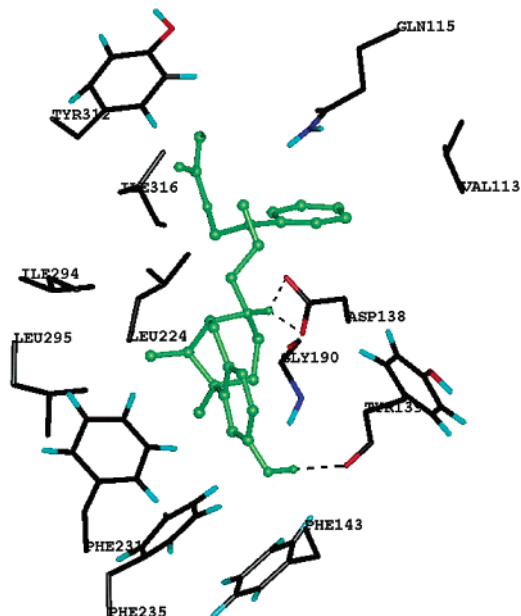


**Figure 12.** Main interaction between the synthetic ligand **2a** and the  $\kappa$ -opioid receptor. Only amino acids located within 5 Å distance from any atom at the bound ligand are displayed and labeled.

phan and the phenyl ring of cyclopropane are stabilized by nonpolar aromatic and nonaromatic residues Phe143 (TM III), Phe231 (TM V), Phe235 (TM V), Ile294 (TM VI), Leu295 (TM VI), Val113 (TM III), and Leu224 (TM V).

## Discussion

The simulations presented in this work provide the first detailed study of molecular dynamics of a  $\kappa$ -opioid receptor inserted into a phospholipid bilayer. This allowed us to operate the simulations at conditions closer to conditions of the natural environment and to gain insight into structural and motional behavior of  $\alpha$ -helices within an explicit DPPC bilayer.

The  $\kappa$ -opioid receptor model retains a largely  $\alpha$ -helical conformation when inserted into a lipid bilayer, and during 500 ps of molecular dynamics simulation, the system remains stable. No constraints on the protein are necessary when solvent and lipids are included.

The analysis of the results of the dynamics simulation of the two different systems, protein–endogenous ligand and protein–synthetic ligands, provided further evidence for the existence of different binding domains for peptide and non-peptide ligands.<sup>44</sup> In fact, the C-terminal parts of TM VI and VII and EL2, as a binding site of the peptide ligand, are essential for high binding affinity of dynA, while the binding site of the synthetic ligands is located deeper inside the receptor on the extracellular side of the transmembrane between helices III, IV, V, VI, and VII. Mutagenesis studies and the recent construction of the GPCR receptor, activated solely by synthetic ligands (RASSL), by Conklin, confirmed these findings.<sup>45</sup> Since the RASSL receptors have no loops in their structure, the seven transmembrane domains are connected by short amino acid sequences only. It was shown that the RASSL receptor is unable to bind the endogenous ligand because of the lack of an EL2 loop. Nevertheless, this receptor keeps its activity when it interacts with small molecules.

This work has revealed similarities in the dynamics and binding modes of all conformations of the synthetic ligands studied. It was found that the protonated hydrogen of the benzomorphan fragment is always involved in an H-bond with Asp138 (TM III). This interaction is typical of all active opioid ligands and represents an essential requisite for the agonist receptor association. The remaining part of the ligand is located in the extracellular portion of the pocket and interacts with different sets of residues of TM III, TM IV, TM V, TM VI, and TM VII. This result is consistent with mutagenesis studies that have highlighted the importance of all transmembrane domains for synthetic ligands with  $\kappa$ -opioid receptor affinity.<sup>46</sup>

The complementary between the groups with similar polarities of the ligands and their binding pocket in the receptor models have been observed. Polar groups of the ligands form H-bonds with the corresponding polar side chains within the binding pocket, and nonpolar groups (aliphatic and aromatic) of ligands make contact with nonpolar side chains of the receptor model through hydrophobic interaction. Some of the hydrophobic residues involved in the ligand binding are unique for the  $\kappa$ -receptor.

The other important finding is that the fluid phase hydrated lipid bilayer membrane can be simulated in conjunction with the protein. Even though the starting point of the construction of the bilayer was an X-ray crystal structure, a liquid-crystalline phase was obtained after the initial preequilibration by a short MD run (99 ps) at the end of the simulations, as shown by rms values (Figure 9) and by hydrocarbon tail order parameters (Figure 10). The construction method appears to have shortened the simulation time needed to equilibrate the system and to reach the liquid-crystalline state. The large differences between the rms values of the lipids and their initial starting structure confirms the change in the lipid conformation. The simulation results were compared with available experimental data of the structure of fluid membranes. Specifically, the hydrocarbon chain deuterium order parameters agree reasonably well with experimental results.

The interactions between individual amino acids of the  $\kappa$ -opioid receptor and lipid or water molecules were investigated. It was found that the amino acids close to the water-lipids interfaces, which are located at the ends of the helices or at EL2, are placed in such a way that the hydrophobic or polar side chains can interact with the hydrocarbon chains of the membrane or with water molecules, respectively. This may be an important factor in the folding and in the stability of secondary and tertiary structural elements of membrane proteins.

## Conclusion

This work has demonstrated that MD simulations of the  $\kappa$ -opioid receptor with its ligands including a lipid bilayer plus water enable unrestrained simulations of the receptor model to be carried out in a realistic model of its natural environment.

The simulations were analyzed in terms of average structure, energetics, and dynamics. Throughout the trajectories, the structure of the protein-membrane complex remained stable. Analysis of the configurational evolution of the DPPC molecules indicates that the

simulated system adopted conformations characteristic of the fluid state. The simulations were tested against several experimental measures of the structure of fluid membranes, such as order parameters, amount of water associated with the phospholipid, and thickness of the membrane. The agreement between parameters measured experimentally and calculated for the computer models reported here was acceptable.

By use of molecular modeling methods, it was possible to deduce the receptor-bound conformations and the binding mode of endogenous as well as synthetic ligands. These findings have confirmed, according to the literature, that the  $\kappa$ -opioid receptor has differential binding domains for peptide and non-peptide ligands. It was found that Asp138 carboxylate (TM III) forms an H-bond with the protonated nitrogen of both classes of ligands. The hydroxyl substituent on the benzomorphan may form an H-bond with Tyr139 (TM III) or Gly190 (TM IV) according to the different molecules. Furthermore, Gln115 (TM II) and Tyr312 (TMVII) are implicated in H-bonding with the carbonyl portion of the synthetic ligands. As part of these specific point interactions, the ligands are surrounded by hydrophobic residues in the transmembrane domains, and consequently, they interact with a different set of residues belonging to all helices.

**Acknowledgment.** Manuela Iadanza thanks Prof. H.-D. Höltje for his comments and support throughout the course of this work during a stay at his laboratories (Heinrich-Heine-Universität, Institute of Pharmaceutical Chemistry, Düsseldorf). She also acknowledges the helpful contributions of Dr. Monika Höltje and Birte Brandt, who made their experience with lipid simulations available. Their assistance is especially appreciated.

## References

- (1) Chen, Y.; Mestek, A.; Liu, J.; Yu, L. Molecular Cloning of a Rat Kappa Opioid Receptor Reveals Sequence Similarities to the Mu and Delta Opioid Receptor. *Biochem. J.* **1993**, *295*, 625–628.
- (2) Guderman, T.; Neurnberg, B.; Schultz, G. Receptors and G-proteins as primary components of transmembrane signal transduction. *J. Mol. Med.* **1995**, *73*, 51–63.
- (3) Ballesteros, J. A.; Weinstein, H. Integrated methods for the construction of three-dimensional models and computation probing of structure-function relations in G-protein coupled receptors. *Methods Neurosci.* **1994**, *25*, 366–428.
- (4) Donnelly, D.; Findlay, J. B. C.; Blundell, T. L. The evolution at structure of aminergic G protein-coupled receptors. *Recept. Channels* **1994**, *2*, 61–78.
- (5) Metzger, T. M.; Paterlini, M. G.; Portoghese, P. S.; Ferguson, D. M. Application of the Message-Address Concept of the Docking of Naltrexone and Selective Naltrexone-Derived Opioid Antagonists into Opioid Receptor Models. *Neurochem. Res.* **1996**, *21*, 1287–1294.
- (6) Metzger, T. M.; Paterlini, M. G.; Portoghese, P. S.; Ferguson, D. M. An Analysis of the Conserved Residues between Halobacterial Retinal Proteins and G-Protein Coupled Receptors: Implications for GPCR Modeling. *J. Chem. Inf. Comput. Sci.* **1996**, *36*, 857–861.
- (7) Schertler, G. F. X.; Villa, C.; Henderson, R. Projection Structure of Rhodopsin. *Nature* **1993**, *362*, 770–772.
- (8) Baldwin, J. M. The Probable Arrangement of the Helices in G Protein-Coupled Receptors. *EMBO J.* **1993**, *12*, 1693–1703.
- (9) Baldwin, J. M.; Schertler, G. F. X.; Unger, V. M. An Alpha-Carbon Template for the Transmembrane Helices in the Rhodopsin Family of G Protein-Coupled Receptors. *J. Mol. Biol.* **1997**, *272*, 144–164.
- (10) Palczewski, K.; Kumasaka, T.; Hori, T.; Behnke, C. A.; Motoshima, H.; Fox, B. A.; Le Trong, I.; Teller, D. C.; Okada, T.; Stenkamp, R. E.; Yamamoto, M.; Miyano, M. Crystal Structure of Rhodopsin: A G Protein-Coupled Receptor. *Science* **2000**, *289*, 739–745.



- (11) Iadanza, M. Synthesis of Non-Peptide Ligands for  $\kappa$  Opioid Receptors; Structure-Affinity Relationships. Ph.D. Thesis, University of Catania, Catania, Italy, 1996.
- (12) Laskowski, R. A.; MacArthur, M. W.; Mass, D. S.; Thornton, J. M. M PROCHECK: A program to check the stereochemical quality of protein structures. *J. Appl. Crystallogr.* **1993**, *26*, 283–291.
- (13) Ronsisvalle, G.; Pasquinucci, L.; Pappalardo, M. S.; Vittorio, F.; Fronza, G.; Romagnoli, C.; Pistacchio, E.; Spampinato, S.; Ferri, S. Non-Peptide Ligands for Opioid Receptors. Design of  $\kappa$ -Specific Agonist. *J. Med. Chem.* **1993**, *36*, 1860–1865.
- (14) Tessmer, M. R.; Kallick, D. A. NMR and Structural Model of Dynorphin A-(1–17) Bound to Dodecylphosphocholine Micelles. *Biochemistry* **1997**, *36*, 1971–1981.
- (15) Sybyl Molecular Modeling System, version 6.4; Tripos Associates: St. Louis, MO.
- (16) Vinter, J. G.; Davis, A.; Saunder, M. R. Strategic Approaches to Drug Design. An Integrated Software Framework for Molecular Modelling. *J. Comput.-Aided Mol. Des.* **1987**, *1*, 31–55.
- (17) Dewar, M. J. S.; Zoebisch, E. G.; Healy, E. F.; Steward, J. J. P. Development and Use of Quantum Mechanical Molecular Models. 76. AM1: A New General Purpose Quantum Mechanical Molecular Model. *J. Am. Chem. Soc.* **1985**, *107*, 3902–3909.
- (18) Clark, M.; Cramer, R. D., III.; Van Opdenbosch, N. Validation of the General Purpose Tripos 5.2 Force Field. *J. Comput. Chem.* **1989**, *10*, 982–1012.
- (19) Maurhofer, E.; Konformationsuntersuchungen an Calciumantagonistisch wirksamen Diphenylalkylaminen, Diphenylbutylpiperidinen, Phenylalkylaminen und Perhexilin. Ph.D. Thesis, Freie Universität Berlin, Berlin, Germany, 1989.
- (20) Paterlini, M. G.; Portoghese, P. S.; Ferguson, D. M. Molecular Simulation of Dynorphin A-(1–10) Binding to Extracellular Loop 2 of the  $\kappa$ -Opioid Receptor. A Model for Receptor Activation. *J. Med. Chem.* **1997**, *40*, 3254–3262.
- (21) Kong, H. Y.; Raynor, K.; Reisine, T. Amino Acids in the Cloned Kappa Receptor That Are Necessary for the High Affinity Agonist Binding but Not Antagonist Binding. *Regul. Pept.* **1994**, *54*, 155–156.
- (22) Surratt, C. K.; Johnson, P. S.; Moriwaki, A.; Seidleck, B. K.; Blaschak, C. J.; Wang, J. B.; Uhl, G. R.  $\mu$ -Opioid Receptor. Charged Transmembrane Domain Amino Acids Are Critical for Agonist Recognition and Intrinsic Activity. *J. Biol. Chem.* **1994**, *269*, 20548–20553.
- (23) Elder, M.; Hitchcock, P. B.; Mason, R.; Shipley, G. G. A Refinement Analysis of the Crystallography of the Phospholipid, 1,2-Dilauroyl-DL-phosphatidylethanolamine, and Some Remarks on Lipid-Lipid and Lipid-Protein Interactions. *Proc. R. Soc. London, Ser. A* **1997**, *354*, 157–170.
- (24) Allen, F. H.; Bellard, S.; Brice, M. D.; Cartwright, B. A.; Doubleday, A.; Higgs, H.; Hummelink, T.; Hummelink-Peters, B. G.; Kennard, O.; Motherwell, W. D. S.; Rodgers, J. R.; Watson, D. G. The Cambridge Crystallographic Data Centre: Computer-Based Search, Retrieval, Analysis and Display of Information. *Acta Crystallogr.* **1979**, *B35*, 2331–2339.
- (25) Pascher, I.; Lundmark, M.; Nyholm, P. G.; Sundell, S. Crystal structures of membrane lipids. *Biochim. Biophys. Acta* **1992**, *1113*, 339–373.
- (26) Hauser, H.; Pascher, I.; Pearson, R. H.; Sundell, S. Preferred Conformation and Molecular Packing of Phosphatidylethanolamine and Phosphatidylcholine. *Biochim. Biophys. Acta* **1981**, *650*, 21–51.
- (27) Pastor, R. W. Molecular Dynamics and Monte Carlo Simulations of Lipid Bilayers. *Curr. Opin. Struct. Biol.* **1994**, *4*, 486–492.
- (28) Heller, H.; Schaefer, M.; Schulten, K. Molecular Dynamics Simulations of a Bilayer of 200 Lipids in the Gel and in the Liquid-Crystal Phases. *J. Phys. Chem.* **1993**, *97*, 8343–8360.
- (29) Tieleman, D. P.; Berendsen, H. J. C. Molecular Dynamics Simulations of a Fully Hydrated Dipalmitoylphosphatidylcholine Bilayer with Different Macroscopic Boundary Conditions and Parameters. *J. Chem. Phys.* **1996**, *105*, 4871–4880.
- (30) Tieleman, D. P.; Berendsen, H. J. C. A Molecular Dynamics Study of the Pores Formed by *Escherichia coli* OmpF Porin in a Fully Hydrated Dipalmitoylphosphatidylcholine Bilayer. *Biophys. J.* **1998**, *74*, 2786–2801.
- (31) Ulrich, A. S.; Volke, F.; Watts, A. The Dependence of Phospholipid Head-Group Mobility on Hydration As Studied by Deuterium-NMR Spin-Lattice Relaxation Time Measurements. *Chem. Phys. Lipids* **1990**, *55*, 61–66.
- (32) Bechinger, B.; Seeling, J. Conformational Changes of the Phosphatidylcholine Headgroup Due to Membrane Dehydration. A  $^2\text{H}$  NMR Study. *Chem. Phys. Lipids* **1991**, *58*, 1–5.
- (33) GROMACS, version 1.6; BIOSON Research Institute, Department of Biophysical Chemistry: University of Groningen, The Netherlands.
- (34) Berendsen, H.; van der Spoel, D.; van Drunen, R. GROMACS: A Message-Passing Parallel Molecular Dynamics Implementation. *Comput. Phys. Commun.* **1995**, *91*, 43–56.
- (35) Ryckaert, J. P.; Bellemans, A. Molecular Dynamics of Liquid *n*-Butane near Its Boiling Point. *Chem. Phys. Lett.* **1975**, *30*, 123–125.
- (36) Ryckaert, J. P.; Bellemans, A. Molecular Dynamics of Liquid Alkanes. *Faraday Discuss. Chem. Soc.* **1978**, *66*, 95–106.
- (37) Berendsen, H. J. C.; Postma, J. P. M.; van Gunsteren, W. F.; DiNola, A.; Haak, J. R. Molecular Dynamics with Coupling to an External Bath. *J. Chem. Phys.* **1984**, *81*, 3684–3689.
- (38) Peyday-Peyroula, E.; Rummel, G.; Rosenbusch, J. P.; Landau, E. M. X-Ray Structure of Bacteriorhodopsin at 2.5 Angstroms from Microcrystals Grown in Lipid Cubic Phases. *Science* **1997**, *277*, 1676–1681.
- (39) Marrik, S. J.; Berger, O.; Tieleman, D. P.; Jahnig, F. Adhesion Forces of Lipids in a Phospholipid Membrane Studied by Molecular Dynamics Simulations. *Biophys. J.* **1998**, *74*, 931–943.
- (40) Berger, O.; Edholm, O.; Jahnig, F. Molecular Dynamics Simulations of a Fluid Bilayer of Dipalmitoylphosphatidylcholine at Full Hydration, Constant Pressure, and Constant Temperature. *Biophys. J.* **1997**, *72*, 2002–2013.
- (41) Egberts, E.; Marrink, S. J.; Berendsen, H. J. C. Molecular Dynamics Simulation of a Phospholipid Membrane. *Eur. Biophys. J.* **1994**, *22*, 423–436.
- (42) Egberts, E.; Berendsen, H. J. C. Molecular Dynamics Simulation of a Smectic Liquid Crystal with Atomic Detail. *J. Chem. Phys.* **1988**, *89*, 3718–3732.
- (43) Seelig, A.; Seelig, J. The dynamic structure of fatty acyl chains in a phospholipid bilayer measured by deuterium magnetic resonance. *Biochemistry* **1974**, *13*, 4839–4845.
- (44) Xue, J. C.; Chen, C.; Zhu, J.; Kunapuli, S. P.; DeRiel, J. K.; Yu, L.; Liu-Chen, L. Y. Differential Binding Domains of Peptide and Non-Peptide Ligands in the Cloned Rat  $\kappa$ -Opioid Receptor. *J. Biol. Chem.* **1994**, *269*, 30195–30199.
- (45) Conklin, B. Presented at IBC's Fourth Annual International Conference on G Protein Coupled Receptors, Orlando, FL, 1998.
- (46) Metzger, T. G.; Ferguson, D. M. On the Role of Extracellular Loops of Opioid Receptors in Conferring Ligand Selectivity. *FEBS Lett.* **1995**, *375*, 1–4.

JM0209127